JNI JOURNAL OF NEUROINFLAMMATION

**RESEARCH**                                                                                    **Open Access**

# Inhibition of metabotropic glutamate receptor 5 induces cellular stress through pertussis toxin-sensitive $G_i$-proteins in murine BV-2 microglia cells

Boonrat Chantong[2], Denise V Kratschmar[1], Adam Lister[1] and Alex Odermatt[1*]

## Abstract

**Background:** Activation of metabotropic glutamate receptor 5 (mGluR5) by (RS)-2-chloro-5-hydroxyphenylglycine (CHPG) was shown to suppress microglia activation and decrease the release of associated pro-inflammatory mediators. In contrast, the consequences of mGluR5 inhibition are less well understood. Here, we used BV-2 cells, retaining key characteristics of primary mouse microglia, to examine whether mGluR5 inhibition by 2-methyl-6-(phenylethynyl)-pyridine (MPEP) enhances cellular stress and production of inflammatory mediators.

**Methods:** BV-2 cells were treated with MPEP, followed by determination of cellular stress using fluorescent dyes and high-content imaging. The expression of inflammatory mediators, endoplasmic reticulum (ER)-stress markers and phosphorylated AMPKα was analyzed by quantitative PCR, ELISA and Western blotting. Additionally, phospholipase C (PLC) activity, cellular ATP content and changes in intracellular free $Ca^{2+}$ ($[Ca^{2+}]_i$) were measured using luminescence and fluorescence assays.

**Results:** Treatment of BV-2 microglia with 100 μM MPEP increased intracellular reactive oxygen species (ROS), mitochondrial superoxide, mitochondrial mass as well as inducible nitric oxide synthase (iNOS) and IL-6 expression. Furthermore, MPEP reduced cellular ATP and induced AMPKα phosphorylation and the expression of the ER-stress markers CHOP, GRP78 and GRP96. The MPEP-dependent effects were preceded by a rapid concentration-dependent elevation of $[Ca^{2+}]_i$, following $Ca^{2+}$ release from the ER, mainly via inositol triphosphate-induced receptors (IP$_3$R). The MPEP-induced ER-stress could be blocked by pretreatment with the chemical chaperone 4-phenylbutyrate and the $Ca^{2+}$ chelator BAPTA-AM. Pretreatment with the AMPK agonist AICAR partially abolished, whilst the inhibitor compound C potentiated, the MPEP-dependent ER-stress. Importantly, the PLC inhibitor U-73122 and the $G_i$-protein inhibitor pertussis toxin (PTX) blocked the MPEP-induced increase in $[Ca^{2+}]_i$. Moreover, pretreatment of microglia with AICAR, BAPTA-AM, U-73122 and PTX prevented the MPEP-induced generation of oxidative stress and inflammatory mediators, further supporting a role for $G_i$-protein-mediated activation of PLC.

**Conclusions:** The results emphasize the potential pathophysiological role of mGluR5 antagonism in mediating oxidative stress, ER-stress and inflammation through a $Ca^{2+}$-dependent pathway in microglia. The induction of cellular stress and inflammatory mediators involves PTX-sensitive $G_i$-proteins and subsequent activation of PLC, IP$_3$R and $Ca^{2+}$ release from the ER.

**Keywords:** Microglia, Glutamate receptor, mGluR5, Inflammation, Oxidative stress, Endoplasmic reticulum stress, Intracellular calcium

* Correspondence: alex.odermatt@unibas.ch
[1]Division of Molecular and Systems Toxicology, Department of Pharmaceutical Sciences, University of Basel, Klingelbergstrasse 50, 4056 Basel, Switzerland
Full list of author information is available at the end of the article

## Background

Neuroinflammation involves the activation and recruitment of immune cells, including microglia, macrophages and lymphocytes, as well as an expression of factors designed to respond to injury and aid in repair. Microglia are resident immune cells in the central nervous system and play an integral role in the neuroinflammatory response. However, excessive microglial activation is a hallmark of neurodegenerative diseases [1].

Metabotropic glutamate receptors (mGluRs) are expressed in many different cell types throughout the brain and spinal cord [2]. They have been considered as promising targets for neuro-protective agents in acute and chronic neurodegenerative disorders [3,4]. The mGluRs are G-protein-coupled receptors (GPCRs) consisting of eight subtypes divided into three groups (I to III) based on their sequence homology, signal transduction pathways and pharmacological profiles [3,5]. The mGluR5 belongs to the group I members, which are typically postsynaptic in neurons and mediate their signaling through Gαq-proteins. Activation results in the stimulation of phospholipase C (PLC) and phosphoinositide hydrolysis, leading to intracellular $Ca^{2+}$ mobilization and activation of extra-cellular signal-regulated kinases 1 and 2 (ERK1/2) downstream signaling pathways [3]. High expression of mGluR5 was found in activated microglia [2,6], which surround the site of injury following traumatic brain injury in rats, suggesting pharmacological mGluR5 manipulation may be beneficial in neuroinflammatory diseases [7,8]. Indeed, the specific mGluR5 agonist (RS)-2-chloro-5-hydroxyphenyl-glycine (CHPG) was shown to inhibit microglial activation, oxidative stress and the release of inflammatory mediators both *in vitro* and *in vivo* [9-14]. Furthermore, the use of agonists to treat chronic spinal cord injuries has been proposed [4]. Thus, a dysregulation resulting in decreased mGluR5 activity may promote the initiation and/or progression of neurodegenerative disorders.

An excessive activation of microglia leads to the enhanced production of ROS and reactive nitrogen species (RNS), which promotes pro-inflammatory pathways via the activation of mitogen-activated protein kinases (MAPKs) and nuclear factor kappa-light-chain-enhancer of activated B cells (NF-κB) [15-18]. The mGluR5 affects ROS and nitric oxide (NO) production through inhibition of NADPH oxidase (NOX-2) activity [9,12-14]; however, the underlying mechanisms are not fully understood. The brain has a high energy demand and therefore depends on efficient mitochondrial function. Impaired mitochondrial dynamics and the chronic generation of ROS and RNS contribute to the pathogenesis of several neurodegenerative diseases [19,20]. A key regulator of mitochondrial adenosine triphosphate (ATP) production is AMP-dependent protein kinase (AMPK), which positively regulates signaling pathways replenishing ATP [21]. Although AMPK is considered

to be a pro-survival kinase, its prolonged activation can induce endoplasmic reticulum (ER)-stress, thereby causing cell damage [22-25]. AMPK is directly targeted and activated by pro-oxidant species and by elevated intracellular $Ca^{2+}$ levels ($[Ca^{2+}]_i$) [23,26], which can result in enhanced MAPK signaling and apoptosis.

Changes in $[Ca^{2+}]_i$ have been implicated in the regulation of several activities of microglia, including proliferation, migration, cytokine release and ROS generation [27-30]. Different stimuli can lead to increased $[Ca^{2+}]_i$, either by $Ca^{2+}$ release from the ER or by entry through the plasma membrane [31]. The ER $Ca^{2+}$ store is regulated by two $Ca^{2+}$ release channels, the inositol triphosphate-induced receptor ($IP_3R$) [32,33] and the ryanodine receptor (RyR) [33], as well as by $Ca^{2+}$ ATPases, which control $Ca^{2+}$ re-uptake into the ER [33]. Both, a prolonged $Ca^{2+}$ depletion in the ER and a $Ca^{2+}$ overload in the cytoplasm can cause ER-stress [34]. Activation of the unfolded protein response (UPR), consisting of the up-regulation of ER-chaperones, attenuation of protein translation and ER-associated degradation of misfolded proteins [35], counteracts ER-stress. The ER-resident molecular chaperones glucose-regulated protein 78 (GRP78) and glucose-regulated protein 94 (GRP94) as well as the transcription factor C/EBP homologous protein (CHOP) are induced by the UPR and they increase ER protein-folding capacity and maintain ER $Ca^{2+}$ stores [35]. Prolonged ER-stress ultimately results in cell death by the apoptotic pathway mediated by caspase-12, an ER localized cysteine protease [35]. In addition to $Ca^{2+}$ homeostasis, impaired mitochondrial function and AMPK signaling modulate the ER-stress response [36-38].

GPCRs play an important role in controlling microglial cell activity. The activation of mGluR5 in microglia has been suggested to involve the Gαq-protein signal transduction pathway through PLC, PKC and $Ca^{2+}$ [10]. Upon stimulation of GPCRs, the inactive Gα-GDP/Gβγ hetero-trimers release GDP and bind GTP, resulting in the dissociation of Gα from Gβγ. The resulting GTP-Gαq complex activates the β-isoforms of PLC [39]. However, a role for pertussis toxin (PTX)-sensitive Gi proteins in $IP_3$ signaling and $[Ca^{2+}]_i$ increase has not, to our knowledge, been reported in microglia.

In order to elucidate the effects of the pharmacological inhibition of mGluR5 on cellular stress and inflammatory mediators in microglia, we tested the responsiveness of BV-2 mouse microglia to the selective mGluR5 antagonist MPEP. There is a close resemblance between BV2 cells and primary mouse microglia in terms of their inflammatory signaling pathways; therefore, BV-2 microglial cells can be used as a model for the activation of microglia *in vitro* [40,41]. In the present study, we show that BV-2 microglia represent a suitable cell model for studying the signaling pathway downstream of mGluR5. Our results provide evidence for a PLC- and $IP_3R$-dependent increase

in $[Ca^{2+}]_i$ following pharmacological mGluR5 inhibition. Importantly, the mGluR5-dependent effects could be blocked by PTX, indicating the involvement of a Gi protein-dependent signal transduction pathway.

## Experimental procedures
### Materials
DMEM, RPMI-1640 medium, penicillin, streptomycin, 0.05% (w/v) trypsin/EDTA, non-essential amino acids (NEAA), 4-(2-hydroxyethyl)-1-piperazineethanesulfonic acid (HEPES), Hank's balanced salt solution (HBSS), EnzChek Direct PLC assay kit, Hoechst-33342, dihydroethidium (DHE), Mitotracker Red CMXRos, MitoSOX Red, Fluo-4 AM and probenecid were obtained from Invitrogen (Carlsbad, CA, USA). FBS was obtained from Connectorate (Dietikon, Switzerland), Cell Titer Glo® assay kit from Promega (Madison, WI, USA) and thapsigargin, AICAR, (RS)-2-chloro-5-hydroxyphenylglycine (CHPG), 6-methyl-2-(phenylethynyl)-pyridine (MPEP), BAPTA-AM, pertussis toxin (PTX), dantrolene sodium and sodium phenylbutyrate (PBA) from Sigma-Aldrich (St. Louis, MO, USA). Compound C and xestospongin C were obtained from Calbiochem (San Diego, CA, USA). Specific antibodies against GRP78, AMPK, and its phosphorylated form were obtained from Cell Signaling Technology (Danvers, MA, USA). Specific antibodies against β-actin and goat anti-rabbit IgG-horseradish peroxidase were obtained from Santa Cruz Biotechnology (Santa Cruz, CA, USA).

### Cell culture and experimental procedure
Murine BV-2 microglia, immortalized by infection with v-raf/c-myc recombinant retrovirus [42], were kindly provided by Professor Wolfgang Sattler, University of Graz, Austria. BV-2 cells were propagated in 75 cm$^2$ flasks in RPMI-1640 medium supplemented with 10% FBS, 2 mM glutamine, 100 μg/mL streptomycin and 100 U/mL penicillin, 10 mM HEPES and 0.1 mM NEAA at 37°C, 5% $CO_2$. Prior to initiating the experiments, cells were resuspended in DMEM supplemented with 10% FBS, 1 g/L glucose, 2 mM glutamine, 100 μg/mL streptomycin and 100 U/mL penicillin, 10 mM HEPES and 0.1 mM NEAA, and seeded again to reach 70% confluence. Cells were then distributed to 96-well ($1 \times 10^3$ cells/well), 24-well ($2 \times 10^4$ cells/well), 12-well ($5 \times 10^5$ cells/well) or 6-well ($1.0 \times 10^6$ cells/well) plates. Cells in the exponential growth phase (60 to 70% confluence) were used for the experiments.

### Determination of mRNA expression
Tri-reagent was used to isolate total RNA according to the manufacturer's instructions (Sigma-Aldrich, St. Louis, MO, USA). Complementary DNA (cDNA) was synthesized from 0.5 μg total RNA using Superscript III reverse transcriptase (Invitrogen, Carlsbad, CA, USA). Briefly, in the first step 0.5 μg of sample RNA and 0.5 μg oligo (dT)15

were made up to a final volume of 12 μL in DNase/RNase-free water in 0.5 mL tubes, which were incubated at 65°C for 5 minutes and immediately transferred to ice. Secondly, reverse transcription reaction mixture (8 μL), containing 4 μL of 5 × first strand buffer (Invitrogen, Carlsbad, CA, USA), 2 μL 0.1 M DTT, 10 U Protector of RNase Inhibitor (Roche Diagnostics, Mannheim, Germany), 0.5 mM dNTP and 20 U Superscript III reverse transcriptase, was added to each sample. Samples were incubated at 42°C for 1 hour. Samples were diluted in DNase/RNase-free water to a working stock of 5 ng/μL of cDNA. Relative mRNA quantification was performed by real-time RT-PCR using a rotor-gene 6000 (Corbett Research, Sydney, Australia). Briefly, the reverse transcriptase was mixed with the cDNA (10 ng), gene-specific primers (200 nM) (Additional file 1: Table S1) and KAPA SYBR FAST qPCR reagent (Kapasystems, Boston, MA, USA) (5 μL), in a final volume of 10 μL. Thermal cycler parameters were as follows: 15 minutes at 95°C, followed by amplification of cDNA for 40 cycles with melting for 15 seconds at 94°C, annealing for 30 seconds at 56°C and extension for 30 seconds at 72°C. For each sample, three replicates were analyzed. Expression was normalized to GAPDH control. Fold changes were quantified as $2^{-(\Delta Ct\ sample - \Delta Ct\ control)}$, as described previously [43].

### Analysis of protein expression
Cells grown in 6-well plates and treated with selected compounds were washed twice with ice-cold PBS and harvested in cold RIPA buffer (Sigma-Aldrich, St. Louis, MO, USA) supplemented with 2% protease inhibitor cocktail (Roche Diagnostics, Mannheim, Germany). Extracts were centrifuged at 10,000 × g for 15 minutes at 4°C in order to remove cell debris.

Protein concentrations were determined using the Pierce® BCA protein assay kit (Thermo Scientific, Waltham, MA, USA) using BSA as protein standard. Absorbance was measured at 595 nm using a UV-max kinetic microplate reader (Molecular Devices, Devon, UK).

Equal amounts of cellular proteins (30 μg/sample) were separated by 10% sodium dodecyl sulfate-polyacrylamide gel electrophoresis (SDS-PAGE) and transferred onto polyvinylidene difluoride (PVDF) membranes (Bio-Rad Laboratories, Hercules, CA, USA) at 120 mA for 1 hour. The membranes were blocked for 1 hour in Tris-buffered saline (TBS), pH 7.4, with 0.1% Tween-20 (TBS-T) containing 10% non-fat milk. The blots were then incubated overnight at 4°C with primary antibodies against AMPKα (D63G4) (1:1,000), phospho-AMPKα (Thr172) (1:1,000), GRP78 (1:500) and β-actin (1:2,000) in TBS-T containing 5% non-fat milk. The membranes were washed 4 × 15 minutes with TBS-T and incubated with goat anti-rabbit IgG-horseradish peroxidase (1:5,000) for 2 hours. After washing the membranes with TBS-T, immunolabeling was

visualized by an enhanced chemiluminescence HRP substrate (Millipore, Billerica, MA, USA) using a Fujifilm LAS-4000 detection system (Bucher Biotec, Basel, Switzerland). β-actin served as loading control of whole cell protein extracts.

### Measurement of intracellular ROS, mitochondrial mass and mitochondrial superoxide by ArrayScan® high-content imaging

Cellular ROS, mitochondrial mass and mitochondrial superoxide were detected using the specific fluorescent dyes dihydroethidium (DHE), MitoTracker®Red CMXRos and MitoSOX Red (Invitrogen, Carlsbad, CA, USA). After the treatments, DHE (10 μg/mL), MitoTracker®Red CMXRos (200 nM) or MitoSOX Red (5 μM) were added to living cells, followed by incubation for 10, 30 and 20 minutes, respectively. Cells were washed twice with PBS, fixed with 4% formaldehyde for 15 minutes and permeabilized by washing twice with 0.1% Triton X-100 in PBS. Nuclei were stained for 30 minutes with 1 μg/mL Hoechst-33342 dissolved in medium. Stained cells were visualized, images captured and the amount of fluorescence was quantified using an ArrayScan® high-content imaging system (Cellomics Inc, Pittsburgh, PA, USA). Fluorescence intensities of each dye were quantified with the cell health profiling bioapplication module. Objects were captured with the appropriate filter on 20 fields, with a total count of approximately 1,000 cells. Cells were identified using Hoechst-33342 dye and a nuclear mask was generated from images of Hoechst-stained nuclei. The values for intracellular ROS, mitochondrial mass and mitochondrial superoxide were expressed as percentage of fluorescence intensity compared with values of the control group.

### PLC activity assay

Phosphatidylcholine-specific PLC activity was determined in whole-cell lysates by using the EnzChek Direct PLC assay (Invitrogen, Carlsbad, CA, USA). Briefly, 100 μL of lysates from treated cells were incubated with 100 μL substrate working solution (glycerol-phosphoethanolamine with a dye-labeled sn-2acyl chain) for 30 minutes and fluorescence was measured at 490 nm excitation and 520 nm emission on a SpectraMax Gemini EM (Molecular Devices, Devon, UK). Enzyme activity was normalized to protein concentration of the respective cell lysate, resulting in mU/μg of protein.

### Measurement of cellular ATP content

Total ATP content was measured by a luminescence-based assay using the CellTiter-Glo® Luminescence assay kit following the manufacturer's instruction (Promega, Madison, WI, USA). The assay buffer and substrate were equilibrated to room temperature. The buffer was transferred and gently mixed with the substrate to obtain a homogeneous solution. After cell treatment, 100 μL of the assay reagent were added into each well and the content was gently mixed under light protection on an orbital shaker to lyse the cells. After 30 minutes, the luminescence was measured on a Microplate Reader (SpectraMax GeminiEM, Molecular Devices, Devon, UK). The luminescence signals for the treated cells were normalized to the luminescence signals from the control group, which was set as 100%.

### Detection of IL-6 by enzyme-linked immunosorbent assay

IL-6 protein secretion in the culture medium of treated BV-2 cells was quantified using a commercially available ELISA kit (BD Biosciences, San Jose, CA, USA). Briefly, 96-well plates (Corning Costar 9018, Sigma-Aldrich, St. Louis, MO, USA) were coated with 50 μL of mouse IL-6 primary antibody in coating buffer and were incubated overnight at 4°C. After washing with PBS-T (PBS containing 0.05% Tween-20), the wells were blocked with 100 μL of assay diluent and incubated for 1 hour, washed, and 100 μL of samples or standards were added. After 2 hours, plates were washed and 50 μL of IL-6 detection antibody diluted 1:250 in assay diluent were added. Plates were incubated for another 1 hour prior to another wash step. The enzyme streptavidin alkaline phosphatase was diluted 1:250 in assay diluent and 50 μL were added per well, followed by incubation for 30 minutes. After washing, 100 μL of substrate solution was added and incubated for 30 minutes in the dark. The reaction was stopped with 50 μL of 1 M $H_3PO_4$ (stop solution), and absorbance was measured at 450 nm with a correction of 570 nm using a UV-max kinetic microplate reader (Molecular Devices, Devon, UK). IL-6 concentrations were calculated from the linear equation derived from the standard curve of known concentrations of purified mouse IL-6.

### Determination of intracellular $Ca^{2+}$ concentrations

Intracellular $Ca^{2+}$ levels were measured with the $Ca^{2+}$-sensitive dye Fluo-4 AM. Cells were stained with 1 μg/mL Hoechst-33342 in medium for 30 minutes. Cells were then washed with HBSS containing 20 mM HEPES and equilibrated with 1 mL loading solution containing with 5 μM Fluo-4 AM, 2.5 mM probenecid and 20 mM HEPES in HBSS for 30 minutes at 37°C, followed by incubation for 30 minutes at room temperature. After loading, cells were washed twice with HBSS to remove excess fluorescent dye. Cells were treated for 1 hour with MPEP or thapsigargin, followed by the subsequent incubation with thapsigargin and MPEP, respectively, for another 1 hour. Alternatively, BV-2 cells were incubated with MPEP with or without dantrolene or xestospongin C in HBSS. The fluorescence intensity of Fluo-4 AM was measured using an ArrayScan® high-content imaging system (Cellomics

Inc). Measurements of fluorescence intensity were captured with appropriate filters on 10 fields, with a total count of approximately 500 cells. Relative changes in $Ca^{2+}$ concentrations were analyzed as a function of time and expressed as $\Delta F/F$ (in %), with F being the baseline fluorescence and $\Delta F$ the variation of fluorescence.

## Statistical analysis

The data represent mean ± SD and were analyzed using one-way ANOVA (V5.00; GraphPad Prism Software Inc., San Diego, CA, USA), followed by a Tukey's *post hoc* test to determine the specific pairs of groups showing statistically significant differences. A *P*-value <0.05 was considered statistically significant.

## Results

### Inhibition of mGluR5 induces inflammatory mediators and cellular stress

Microglia are known to increase their production of inflammatory mediators as well as ROS and RNS upon activation.

In order to investigate the role of mGluR5 on microglial activity, we treated BV-2 mouse microglia with the pharmacological mGluR5 activator CHPG and the inhibitor MPEP and assessed their impact on cellular stress markers and inflammatory mediators. After 24 hours of incubation with 100 μM of the mGluR5 antagonist MPEP, a significant increase (132 ± 5%) of intracellular ROS, detected by DHE, was observed (Figure 1A). Mitochondrial mass, measured by MitoTracker®Red CMXRos, was similarly enhanced (134 ± 6%) (Figure 1B). Mitochondrial superoxide production was assessed using MitoSOX Red, which turned out to be the most sensitive marker for oxidative stress, with an increase of 314 ± 15% upon treatment with MPEP (Figure 1C).

In addition, the mRNA expression of iNOS was determined by quantitative PCR, revealing a three-fold increase following treatment with MPEP (Figure 1D). Furthermore, MPEP enhanced the mRNA and protein levels of the inflammatory cytokine IL-6 by 6- and 29-fold (Figure 1E,F), respectively. The agonist CHPG (100 μM) had no effect
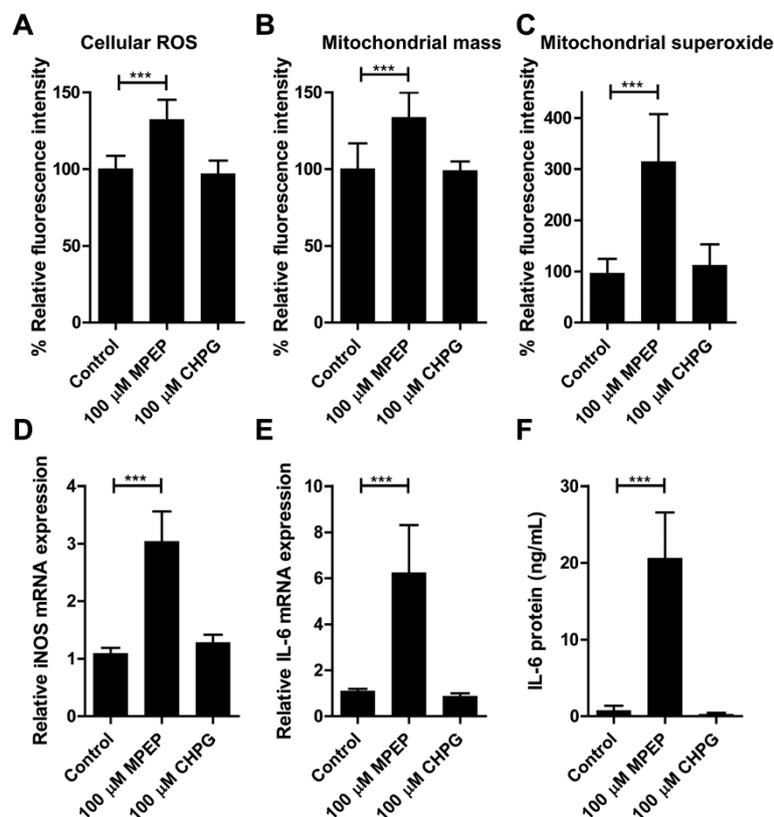


**Figure 1 Increased cellular stress and inflammatory mediators upon inhibition of mGluR5 in BV-2 cells.** BV-2 cells were treated for 24 hours with 100 μM of either CHPG or MPEP. **(A)** Intracellular reactive oxygen species (ROS) levels were determined using dihydroethidium (DHE). **(B)** Mitochondrial mass was measured using MitoTracker®Red CMXRos. **(C)** Mitochondrial superoxide levels were determined using MitoSOX Red. The expression of inducible nitric oxide synthase (iNOS) mRNA **(D)** and IL-6 mRNA **(E)** were measured by quantitative PCR. Results are expressed relative to the values of the house-keeping control GAPDH. **(F)** IL-6 protein levels were determined by ELISA. Results represent mean ± SD of three independent experiments. Significance was analyzed by one-way ANOVA followed by Tukey's test. ***$P$ <0.005. CHPG, (RS)-2-chloro-5-hydroxyphenylglycine; GAPDH, glyceraldehyde 3-phosphate dehydrogenase; MPEP, 2-methyl-6-(phenylethynyl)-pyridine.

on oxidative stress markers and inflammatory mediators in non-induced BV-2 cells.

### Blocking mGluR5 causes ATP depletion and results in AMPK activation

Enhanced cellular stress is often associated with changes in ATP levels. Therefore, we measured the intracellular ATP content in BV-2 cells incubated with 100 μM MPEP. A time-dependent decrease of total ATP content was observed, reaching significance as early as 1 hour after exposure to MPEP ($16 \pm 1\%$ lower ATP level) (Figure 2A). As shown in Figure 2B, treatment of cells for 2 hours with 100 μM MPEP resulted in approximately 40% decreased cellular ATP levels compared with control cells. Treatment with 1 μM compound C lowered ATP levels. As expected, pretreatment of the cells with compound C potentiated the effect of MPEP to reduced ATP levels. In contrast, 1 mM of the AMPK activator AICAR tended to increase ATP levels ($133 \pm 7\%$ compared with control), and pretreatment of cells with AICAR completely reversed the ATP depletion observed upon incubation with MPEP alone.

To further examine the stimulation of AMPK activation by MPEP, the phosphorylation of the AMPKα subunit was measured by immunoblotting following treatment with the chemicals indicated for 0.5, 1 and 2 hours (Figure 2C). The signal obtained for phosphorylated AMPKα was increased after 1 hour of incubation with 100 μM MPEP. The positive control (1 mM AICAR) was slightly more efficient and led to a trend increase of AMPKα phosphorylation already after 0.5 hours of incubation. AMPK phosphorylation further increased when the cells were treated with either AICAR or MPEP for 2 hours, reaching significant difference compared with control. As shown in Figure 2E,F co-incubation of BV-2 cells with MPEP and AICAR further enhanced AMPKα phosphorylation, whereas compound C was able to reverse the MPEP-induced increase of AMPKα phosphorylation.

### Increased intracellular $Ca^{2+}$ levels following mGluR5 inhibition

Next, we tested whether the observed ATP depletion upon inhibition of mGluR5 was associated with an increased $[Ca^{2+}]_i$.

The effects of MPEP on $[Ca^{2+}]_i$ were determined using the fluorescent indicator Fluo-4 AM. BV-2 cells kept in $Ca^{2+}$-free medium were incubated with 100 μM MPEP
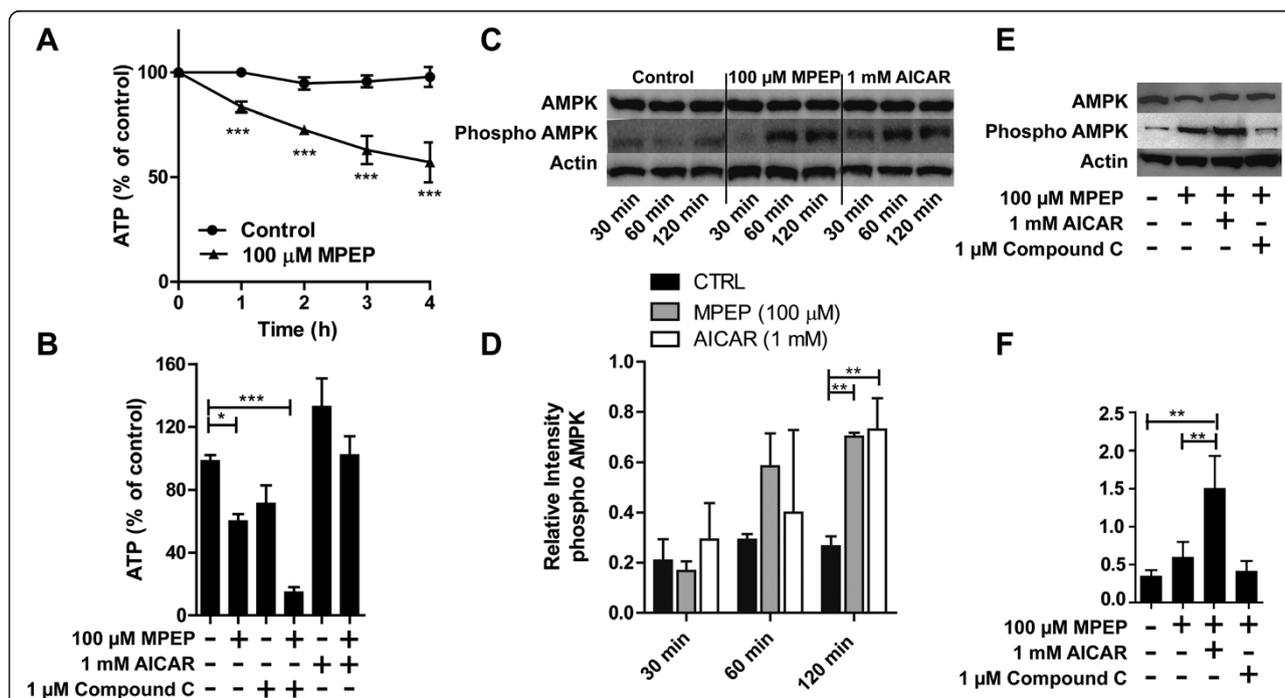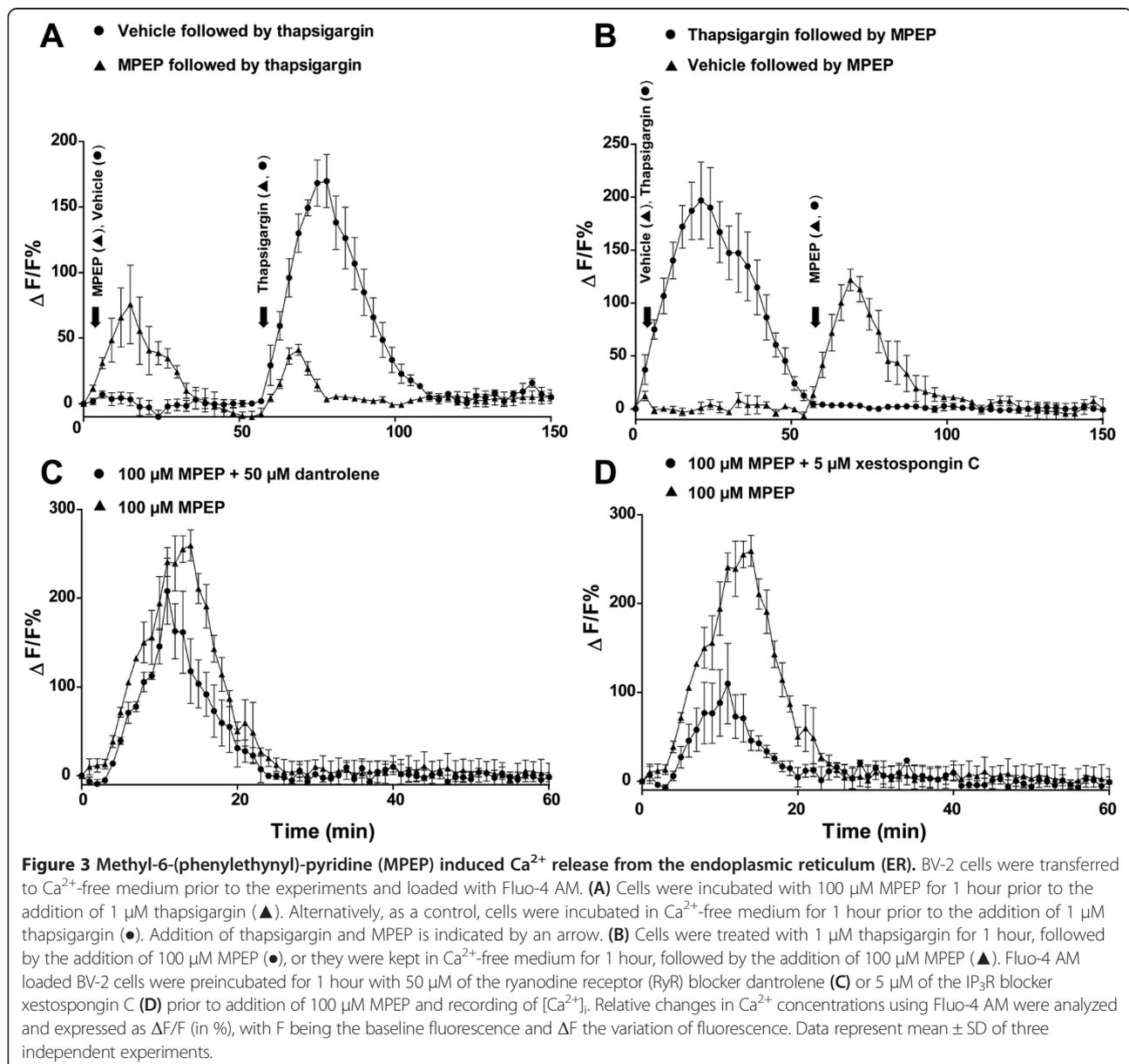


**Figure 2 ATP depletion and activation of AMP-dependent protein kinase (AMPK) caused by inhibition of mGluR5. (A)** BV-2 cells were incubated with 100 μM MPEP for 1, 2, 3 and 4 hours, followed by determination of cellular ATP levels. **(B)** Cells were treated for 2 hours with 100 μM MPEP, 1 μM of the AMPK inhibitor compound C, 1 mM of the AMPK activator AICAR or combinations, followed by determination of cellular ATP content. Results represent mean ± SD of three independent experiments. Significance was tested by one-way ANOVA followed by Tukey's test. *$P$ <0.05, ***$P$ <0.005. **(C)** Immunoblot analyses were performed on lysates of BV-2 cells that had been treated with MPEP or AICAR (positive control) for the indicated time period. **(D)** Densitometric analysis of phospho-AMPK band normalized against β-actin. **(E)** Immunoblot analyses were performed on lysates of BV-2 cells that had been pre-incubated with either AICAR (1 mM) or compound C (1 μM) prior to incubation with MPEP for 2 hours. **(F)** Densitometric analysis of phospho-AMPK band normalized against β-actin. MPEP, 2-methyl-6-(phenylethynyl)-pyridine.

and kinetic $[Ca^{2+}]_i$ changes were analyzed every minute. MPEP significantly increased $[Ca^{2+}]_i$ (Figure 3A). Subsequent addition of the ER $Ca^{2+}$-ATPase inhibitor thapsigargin resulted in only a small increase in $[Ca^{2+}]_i$, compared with cells that were treated with thapsigargin alone, suggesting that the observed MPEP-induced rise in $[Ca^{2+}]_i$ was mainly due to $Ca^{2+}$ release from the ER. As shown in Figure 3B, $[Ca^{2+}]_i$ did no longer respond to MPEP in cells that were pretreated with thapsigargin, indicating that ER $Ca^{2+}$ stores were depleted. To provide initial evidence for the receptor involved in the $Ca^{2+}$ efflux from the ER following exposure to MPEP, we incubated BV-2 cells with the RyR blocker dantrolene [44] or the $IP_3R$ blocker xestospongin C prior to addition of MPEP. While dantrolene had only a minor inhibiting effect on the increase of

$[Ca^{2+}]_i$ by MPEP (Figure 3C), xestospongin C more effectively prevented the MPEP-induced $Ca^{2+}$ release from the ER (Figure 3D), suggesting that $IP_3R$ is the major target of mGluR5-mediated signaling.

## Induction of ER-stress markers upon inhibition of mGluR5

Disturbances in $Ca^{2+}$ homeostasis can trigger ER-stress; therefore we tested whether inhibition of mGluR5 by MPEP induces ER-stress in BV-2 cells. MPEP treatment resulted in a time-dependent increase in GRP78 protein expression (Figure 4A,B). Furthermore, the mRNA expression levels of the ER-stress markers CHOP, GRP78 and GRP94 were significantly increased after exposure to MPEP for 24 hours (3.5-fold, 3.0-fold and 3.8-fold compared with control, respectively) (Figure 4C). To further



**Figure 3 Methyl-6-(phenylethynyl)-pyridine (MPEP) induced Ca²⁺ release from the endoplasmic reticulum (ER).** BV-2 cells were transferred to Ca²⁺-free medium prior to the experiments and loaded with Fluo-4 AM. **(A)** Cells were incubated with 100 μM MPEP for 1 hour prior to the addition of 1 μM thapsigargin (▲). Alternatively, as a control, cells were incubated in Ca²⁺-free medium for 1 hour prior to the addition of 1 μM thapsigargin (●). Addition of thapsigargin and MPEP is indicated by an arrow. **(B)** Cells were treated with 1 μM thapsigargin for 1 hour, followed by the addition of 100 μM MPEP (●), or they were kept in Ca²⁺-free medium for 1 hour, followed by the addition of 100 μM MPEP (▲). Fluo-4 AM loaded BV-2 cells were preincubated for 1 hour with 50 μM of the ryanodine receptor (RyR) blocker dantrolene **(C)** or 5 μM of the IP₃R blocker xestospongin C **(D)** prior to addition of 100 μM MPEP and recording of [Ca²⁺]ᵢ. Relative changes in Ca²⁺ concentrations using Fluo-4 AM were analyzed and expressed as ΔF/F (in %), with F being the baseline fluorescence and ΔF the variation of fluorescence. Data represent mean ± SD of three independent experiments.

**Figure 4 Induction of endoplasmic reticulum (ER)-stress markers by blockage of mGluR5. (A)** Immunoblot analyses to detect GRP78 protein were performed on lysates of BV-2 cells that had been treated with 100 μM MPEP for the indicated time period. β-actin served as a loading control. **(B)** Densitometric analysis of GRP78 band normalized against β-actin. **(C)** Cells were preincubated for 1 hour with 1 μM BAPTA-AM or 1 mM sodium phenylbutyrate (PBA), followed by further incubation with 100 μM MPEP for 24 hours. Expression of CHOP, GRP78 and GRP94 mRNA were measured by quantitative PCR. **(D)** Cells were pre-exposed for 1 hour with 1 mM AICAR or 1 μM compound C, followed by a further incubation with 100 μM MPEP for 2 hours and GRP78 protein levels were analyzed by immunoblotting. **(E)** Densitometric analysis of GRP78 band normalized against β-actin. **(F)** Cells were pre-exposed for 1 hour with 1 mM AICAR or 1 μM compound C, followed by a further incubation with 100 μM MPEP. Expression of CHOP, GRP78 and GRP94 mRNA were measured by quantitative PCR and mRNA expression levels were normalized to GAPDH control. Results represent mean ± SD of three independent experiments. Significance was analyzed by one-way ANOVA followed by Tukey's tests. **$P <0.01$; ***$P <0.005$. CHOP, C/EBP homologous protein; GAPDH, glyceraldehyde 3-phosphate dehydrogenase; MPEP, 2-methyl-6-(phenylethynyl)-pyridine.

study the impact of MPEP on ER-stress, we pretreated cells for 1 hour with 1 mM of the chemical chaperone 4-phenylbutyrate (4-PBA), followed by incubation with MPEP for 24 hours. The MPEP-induced increase in the mRNA expression of the major ER-stress markers was almost fully prevented by 4-PBA (Figure 4C). To test whether the rise in $[Ca^{2+}]_i$ contributes to the increased expression of the ER-stress markers, we pretreated BV-2 cells for 1 hour with 1 μM of the $Ca^{2+}$ chelator BAPTA-AM prior to further incubation in the presence of 100 μM MPEP for 24 hours. Pretreatment of cells with BAPTA-AM abolished the induction of the expression of the three ER-stress markers, indicating that the rise in $[Ca^{2+}]_i$ is a critical step in the cellular stress response to mGluR5 inhibition.

To evaluate whether the effect of MPEP on ER-stress involves AMPK, we examined the effect of AICAR and compound C on GRP78 protein expression. Cells were pretreated with either AICAR (1 mM) or compound C (1 μM) for 1 hour, followed by incubation with MPEP (100 μM) for 2 hours. AICAR or compound C treatment alone did not significantly alter GRP78 protein levels (data not shown). However, compound C potentiated the MPEP-mediated induction of GRP78 expression (Figure 4D,E). In contrast, activation of AMPK activity by AICAR tended to reduce the MPEP-dependent induction of GRP78 protein expression. Furthermore, we determined the impact of pretreatment of the cells with either AICAR (1 mM) or compound C (1 μM) for 1 hour

on the effect of 100 μM MPEP for 24 hours on the mRNA levels of CHOP, GRP78 and GRP94 (Figure 4F). Compound C partially prevented the increase in CHOP, GRP78 and GRP94 mRNA expression levels upon exposure to MPEP, whereas AICAR potentiated the MPEP-stimulated mRNA expression of the ER-stress markers. These findings strongly suggest that AMPK is involved in the MPEP-mediated effects on ER-stress markers in BV-2 cells.

### $Ca^{2+}$ release upon inhibition of mGluR5 is dependent on PLC

Activation of PLC produces $IP_3$, which activates $IP_3R$, thereby inducing $Ca^{2+}$ release from the ER in a variety of cells. Therefore, we investigated a possible role of PLC in the MPEP-dependent $Ca^{2+}$ release from the ER. As shown in Figure 5A, MPEP increased $[Ca^{2+}]_i$ in a concentration-dependent manner. Importantly, pretreatment of cells with 5 μM of the PLC inhibitor U-73122 completely abolished the effect of 100 μM MPEP.
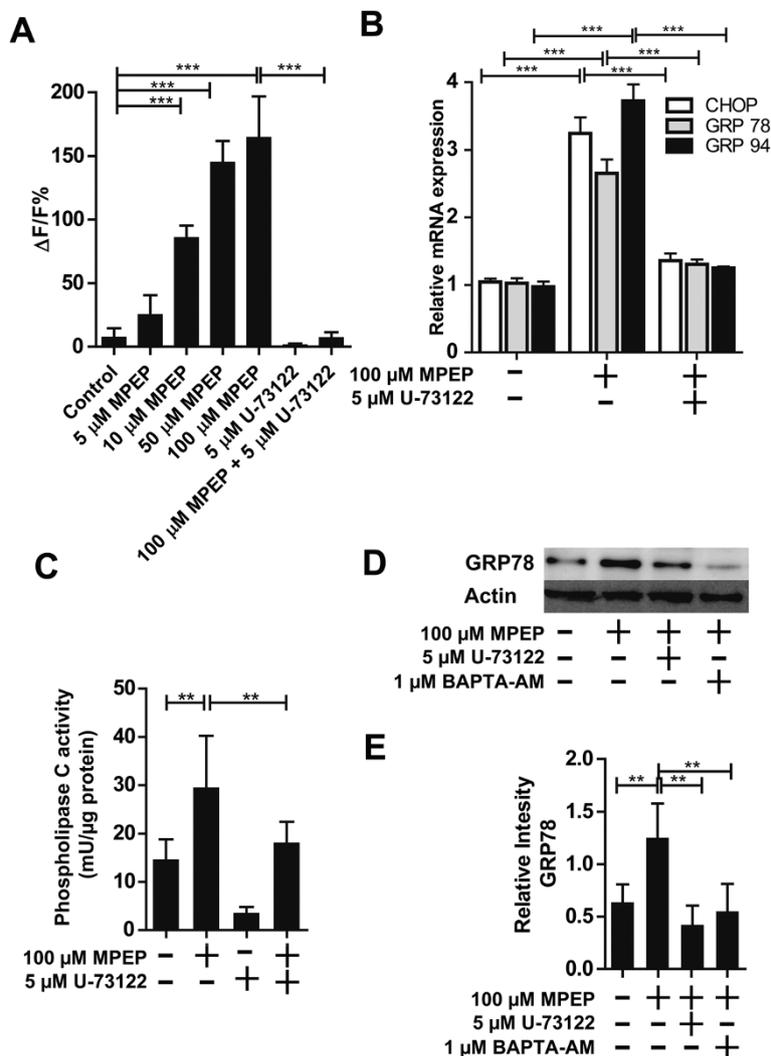


**Figure 5 Activation of phospholipase C (PLC) upon inhibition of mGluR5. (A)** Intracellular $Ca^{2+}$ concentrations were determined by measuring the fluorescence intensity of the fluorochrome Fluo-4 AM. BV-2 cells were pretreated for 1 hour with 5 μM U-73122 prior to the addition of 100 μM MPEP. Relative changes in the $Ca^{2+}$ concentrations detected by Fluo-4 AM were analyzed after 15 minutes. Results are expressed as ΔF/F (in %), with F being the baseline fluorescence and ΔF the variation of fluorescence. Data represent the mean ± SD. **(B)** Cells were incubated for 24 hours with 100 μM MPEP in the presence or absence of 5 μM of the phospholipase C inhibitor U-73122, followed by determination of mRNA expression of CHOP, GRP78 and GRP95 by quantitative PCR. Results were normalized to GAPDH mRNA control. Results represent the mean ± SD from three independent experiments, each performed in triplicate. **(C)**, BV-2 cells were incubated with 100 μM MPEP for 2 hours with or without pretreatment for 1 hour with 5 μM U-73122, followed by determination of PLC activity. PLC activity (mU/μg total protein) is given as the mean ± SD from three independent experiments. **(D)** BV-2 cells were incubated with 100 μM MPEP in the absence or presence of 5 μM PLC inhibitor U-73122 or 1 μM $Ca^{2+}$ chelator BAPTA-AM, followed by the determination of GRP78 protein expression by immunoblotting. **(E)** Densitometric analysis of GRP78 band normalized against β-actin. **$P < 0.01$; ***$P < 0.001$. CHOP, C/EBP homologous protein; GAPDH, glyceraldehyde 3-phosphate dehydrogenase; MPEP, 2-methyl-6-(phenylethynyl)-pyridine.
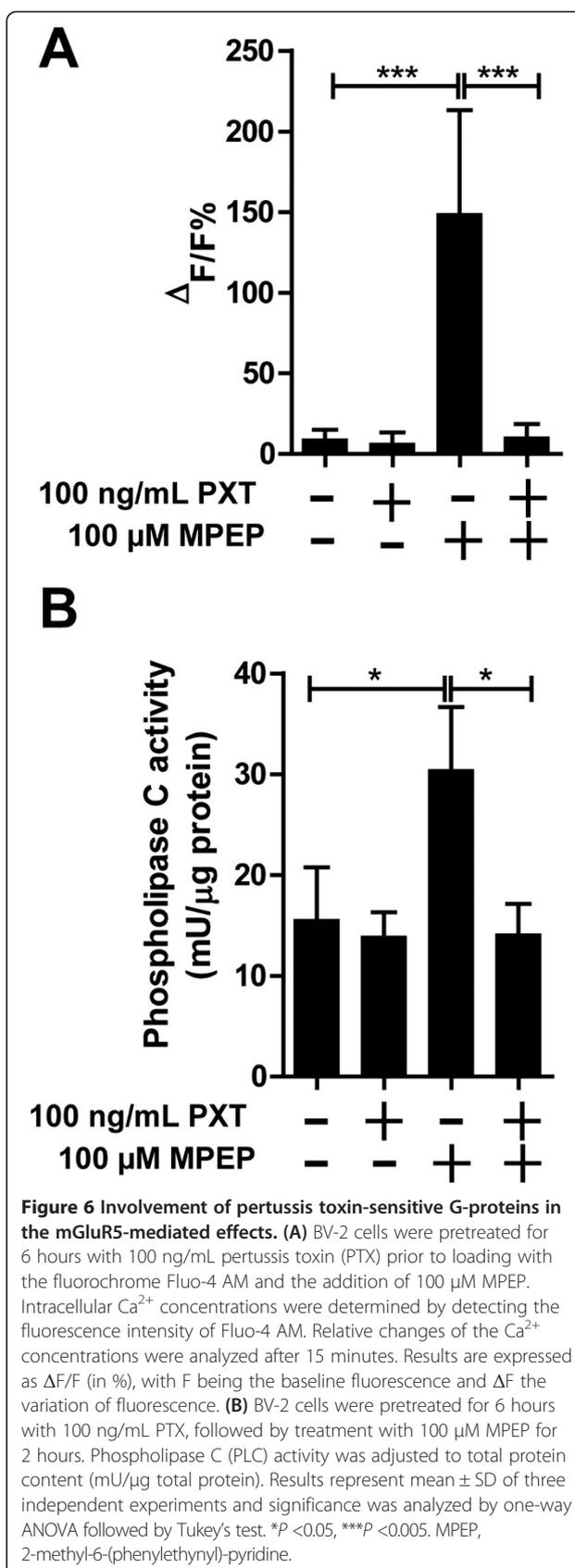
Furthermore, the MPEP-dependent induction of CHOP, GRP78 and GRP96 mRNA expression, measured after 24 hours, was also prevented by cotreatment of the cells with U-73122 (Figure 5B). Next, we investigated whether MPEP leads to enhanced PLC activity. Total PLC activity was significantly increased in cells treated with MPEP for 2 hours compared with control (Figure 5C). The MPEP-induced increase in total PLC activity was completely blocked by pretreatment with U-73122 for 1 hour. U-73122 also significantly decreased basal PLC activity in BV-2 cells. In addition, inhibition of PLC by U-73122 reduced the MPEP-induced up-regulation of GRP78 protein expression (Figure 5D,E). Cotreatment of the cells with BAPTA-AM also abolished the effect of MPEP, indicating that $Ca^{2+}$ is directly involved in the MPEP-dependent induction of ER-stress markers. These results revealed a role for PLC in the MPEP-induced $Ca^{2+}$ elevation and ER-stress.

### Pertussis toxin-sensitive G-protein coupled receptors are involved in the mGluR5-mediated effects

Several studies have demonstrated that G-protein coupled receptors may exert their effects through activation of PLC, which hydrolyzes phospholipids in cell membranes to $IP_3$ and diacylglycerol. To investigate the $[Ca^{2+}]_i$ responses to MPEP, we pretreated cells for 6 hours with 100 ng/mL pertussis toxin (PTX), a specific inhibitor of Gi/o-type G-proteins. As shown in Figure 6A, pretreatment of cells with PTX completely abolished the MPEP-induced increase in $[Ca^{2+}]_i$, suggesting the involvement of Gi/o-proteins in $[Ca^{2+}]_i$ responses to MPEP. Pretreatment of BV-2 cells with PTX prevented the MPEP-dependent activation of PLC, while PTX alone did not affect basal activity of PLC (Figure 6B). These results suggest that MPEP utilizes a PTX-sensitive G-protein in the activation of PLC, which leads to enhanced $[Ca^{2+}]_i$ and activation of ER-stress markers. To further investigate the downstream effects of MPEP after PLC activation and increase in $[Ca^{2+}]_i$, we investigated whether PTX might suppress the MPEP-dependent induction of GRP78 expression. Upon pretreatment of cells for 6 hours with PTX a trend decrease in MPEP-induced GRP78 expression was observed by Western blot analysis; however, the results did not reach significance (data not shown).

### Induction of cellular stress and inflammatory mediators upon mGluR5 inhibition can be prevented by interfering with intracellular signaling

In order to further study the impact of the intracellular signaling pathways that were shown to be influenced by mGluR5 above, we pretreated BV-2 cells with the various modulators and measured the effects of MPEP exposure on the regulation of cellular stress and inflammatory mediators. The levels of intracellular ROS, mitochondrial
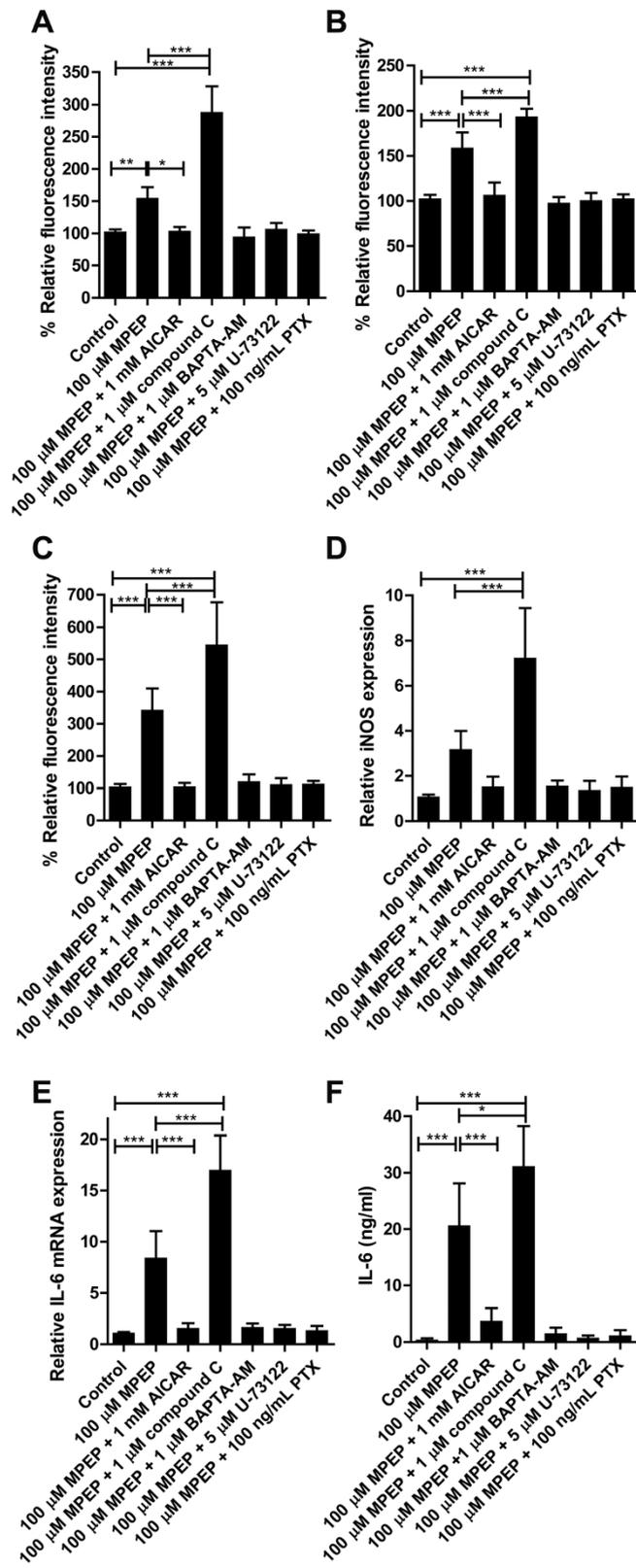


**Figure 6 Involvement of pertussis toxin-sensitive G-proteins in the mGluR5-mediated effects. (A)** BV-2 cells were pretreated for 6 hours with 100 ng/mL pertussis toxin (PTX) prior to loading with the fluorochrome Fluo-4 AM and the addition of 100 μM MPEP. Intracellular $Ca^{2+}$ concentrations were determined by detecting the fluorescence intensity of Fluo-4 AM. Relative changes of the $Ca^{2+}$ concentrations were analyzed after 15 minutes. Results are expressed as ΔF/F (in %), with F being the baseline fluorescence and ΔF the variation of fluorescence. **(B)** BV-2 cells were pretreated for 6 hours with 100 ng/mL PTX, followed by treatment with 100 μM MPEP for 2 hours. Phospholipase C (PLC) activity was adjusted to total protein content (mU/μg total protein). Results represent mean ± SD of three independent experiments and significance was analyzed by one-way ANOVA followed by Tukey's test. *$P$ <0.05, ***$P$ <0.005. MPEP, 2-methyl-6-(phenylethynyl)-pyridine.

**Figure 7** (See legend on next page.)

(See figure on previous page.)

**Figure 7 Prevention of cellular stress and inflammatory mediators by interference with intracellular signaling.** BV-2 cells were pretreated for 1 hour with 1 μM compound C, 1 μM BAPTA-AM or 5 μM U-73122, or for 6 hours with pertussis toxin (PTX) (100 ng/mL) prior to incubation with 100 μM MPEP for 24 hours. **(A)** Intracellular reactive oxygen species (ROS) levels were determined using dihydroethidium (DHE). **(B)** Mitochondrial mass was measured using MitoTracker®Red CMXRos. **(C)** Mitochondrial superoxide levels were detected using MitoSOX Red. The mRNA expression of inducible oxygen species (iNOS) **(D)** and IL-6 **(E)** were determined by quantitative PCR and values were normalized to GAPDH mRNA control. **(F)** IL-6 protein expression was measured by ELISA. Results represent the mean ± SD of at least three independent experiments. Significance was tested by one-way ANOVA followed by Tukey's test. *$P$ <0.05, **$P$ <0.01; ***$P$ <0.005. GAPDH, glyceraldehyde 3-phosphate dehydrogenase; MPEP, 2-methyl-6-(phenylethynyl)-pyridine.

mass, mitochondrial superoxide production, iNOS mRNA as well as IL-6 mRNA and protein were determined. Pretreatment of cells with AICAR reversed the effects of MPEP on cellular stress parameters and cytokine expression, whereas compound C potentiated them (Figure 7). BAPTA-AM, U-73122 and PTX completely abolished the MPEP-dependent induction of ROS production and inflammatory cytokine expression. Together, these data suggest that blockage of mGluR5 by MPEP leads to the activation of PTX-sensitive G-proteins that causes activation of PLC, with subsequent $Ca^{2+}$ release from the ER, thereby producing cellular stress and enhancing the expression of inflammatory cytokines.

## Discussion

Several reports have shown that mGluR5 exerts neuroprotective effects in microglia cells by modulating oxidative stress and inflammatory cytokine release both *in vitro* and *in vivo*. It has been shown that the mGluR5 agonist CHPG diminished NF-κB activation, NADPH oxidase activity and ROS production in lipopolysaccharide (LPS)-stimulated microglia and improved functional recovery after traumatic brain injury [7,8,12]. Delayed CHPG administration suppressed the activation of microglia and chronic neuroinflammation and decreased the hippocampal neuronal loss and lesion progression following experimental traumatic brain injury in mice [9]. Byrnes *et al.* showed that in primary microglia from mGluR5-deficient mice CHPG was no longer able to decrease the LPS-induced inflammation and oxidative stress, indicating a key role for mGluR5 in the modulation of microglial activation [10]. Furthermore, they provided evidence for a role of PLC, PKC and $Ca^{2+}$ in the mGluR5-mediated effects. In contrast to its activation, the possible consequences of the inhibition of mGluR5 by xenobiotics on cellular stress parameters and inflammatory mediators in microglia remains less well understood.

In the present study, we used BV-2 mouse microglia cells, which show highly overlapping gene expression profiles with primary mouse microglia and therefore represent a valuable model system for primary mouse microglia [41], to investigate the effects of the mGluR5 blocker MPEP on cellular stress parameters, inflammatory mediators and the underlying signaling pathways.

Although MPEP is widely used to modulate the mGluR5 receptor it has been reported that the compound lacks sensitivity against mGluR5, leading to off-target effects while antagonizing other receptors. Thus, it has been shown that MPEP exerts neuroprotective effects at high concentrations, mediated by inhibition of the N-methyl-D-aspartate receptor (NMDA) [45]. MPEP, at the concentrations used in the present study, may have off-target effects *in vivo*. Specifically, MPEP has been shown to antagonize the mGluR1 and NR2B receptors [46] and positively regulate the mGluR4 receptor [47]. BV-2 cells express high protein levels of mGluR5 and very low levels of mGluR1 [13]. Additionally, evidence shows that the effect of MPEP on the NR2B and mGluR4 receptor would be neuroprotective [47,48]. Since our results show that MPEP induces cellular stress, we are confident that MPEP is targeting mGluR5; however, contribution of other affected targets to the observed results cannot be excluded. More selective antagonists of mGluR5 receptors such as the recently developed 3-[(2-methyl-1,3-thiazol-4-yl) ethynyl] pyridine (MTEP) might be used to address possible off-target effects. Exposure of BV-2 cells to MPEP increased total and mitochondrial ROS production, caused mitochondrial swelling and enhanced the expression of iNOS as well as the expression and release of IL-6 (Figure 8). CHPG completely reversed the effects of MPEP, indicating that the MPEP-induced oxidative stress and up-regulation of cytokines was mediated by mGluR5 inactivation (data not shown). These results are consistent with previous studies reporting a protective role of microglial mGluR5 activation on neuronal cells and in preventing brain damage [9-12,49].

On the other side, some studies provided evidence for neuroprotective effects of mGluR5 inhibition by MPEP. A prolonged exposure of spinal cord motor neurons to cultures enriched in reactive astrocytes to MPEP reduced AMPA-mediated toxicity and cobalt uptake in motor neurons [50]. The protective effect of MPEP was absent in cultures with low astrocyte numbers, suggesting that blockade of mGluR5 in astrocytes was responsible for the observed effects. Thus, mGluR5 likely exerts differential effects in microglia and astrocytes. Another study showed a neuroprotective effect of MPEP in a rodent 6-hydroxydopamine Parkinson's disease
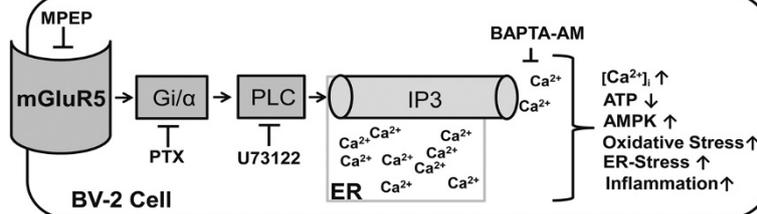
**Figure 8 Schematic presentation of signaling mechanisms and cellular outcomes following mGluR5 blockade.**

model [51]. Their results suggested that enhanced gluta-minergic activity to the substantia nigra pars compacta may contribute to the progression of nigral dopamin-ergic neuronal degeneration and that mGluR5 blockers might delay disease progression. The exact mode of action, however, remained unclear.

To begin to understand why mGluR5 blockade results in enhanced cellular stress in microglia, we investigated the mGluR5-mediated signaling pathway in BV-2 cells upon treatment with MPEP. Our results revealed a rapid increase in $[Ca^{2+}]_i$, with peak concentrations reached 15 minutes after addition of MPEP and return to baseline after 40 minutes. The fact that pre-exposure of cells to thapsigargin completely abolished the MPEP-induced increase in $[Ca^{2+}]_i$, and *vice versa* pre-incubation with MPEP reduced thapsigargin-induced $[Ca^{2+}]_i$ increase, indicated that $Ca^{2+}$ was released from the ER. Furthermore, the IP$_3$R blocker xestospongin C effectively prevented the MPEP-induced $Ca^{2+}$ release from the ER, whereas the RyR antagonist dantrolene was less effective, suggesting a major role for IP$_3$R in the mGluR5-dependent signaling pathway.

Changes in $[Ca^{2+}]_i$ represent a major signaling pathway in microglia. Exposure of microglia to LPS leads to chronically elevated $[Ca^{2+}]_i$ and it was shown that the $Ca^{2+}$ chelator BAPTA-AM could prevent the LPS-induced release of NO and the cytokines TNF-α, IL-6 and IL-12 [52]. Importantly, blockade of IP$_3$R by xestospongin C has been shown to abolish the production of TNF-α and IL-6 in activated microglia [53].

Impaired microglial $Ca^{2+}$-mediated signal transduction was observed under pathological conditions. Exposure to amyloid-β increased $[Ca^{2+}]_i$ in cultured microglia, and basal $[Ca^{2+}]_i$ was higher in microglia isolated from the brain of Alzheimer's patients compared with microglia from non-demented individuals [54,55]. Increased $[Ca^{2+}]_i$ may act directly on the mitochondrial membrane, leading to enhanced ROS production [56,57]. Furthermore, a $Ca^{2+}$ overload decreases mitochondrial function by triggering the opening of the mitochondrial membrane permeability transition pore, resulting in mitochondrial membrane depolarization and swelling, enhanced ROS generation and decreased ATP production [58-60].

Mitochondrial dysfunction and ATP depletion have been associated with increased oxidative stress and neuroinflammation [61-63]. The rapid ATP depletion observed in the present study in BV-2 cells following incubation with MPEP could be caused by excessive ATP consumption by ER $Ca^{2+}$-ATPases attempting to lower $[Ca^{2+}]_i$ by $Ca^{2+}$ reuptake into the ER and/or mitochondrial dysfunction and impaired ATP production. The MPEP-dependent ATP depletion was ameliorated by pretreatment of cells with the AMPK inducer AICAR, indicating an involvement of AMPK in the modulation of the mGluR5-mediated effects. The depletion of ATP is likely to occur prior to the induction of AMPKα phosphorylation, in line with the role of AMPK in restoring cellular ATP levels [64]. Studies in BV-2 microglia and in glial cells have shown that the pharmacological activation of AMPK suppresses the pro-inflammatory responses [65,66]. On the other side, AMPK activation was found to enhance ROS production in microglia and in pancreatic beta-cells exposed to high glucose levels [67-69], and some of the observations may depend on the specific conditions of the respective study. Nevertheless, the results of the present study provide, to our knowledge, the first evidence for an association between mGluR5 inhibition and subsequent ATP depletion and AMPK activation in microglia.

The excessive $Ca^{2+}$ release from the ER may be responsible for the observed ATP depletion. It may further lead to the depletion of ER luminal $Ca^{2+}$ stores, which is believed to trigger ER-stress and activate the UPR pathway, including the induction of the expression of ER chaperones such as CHOP, GRP78 and GRP96 [35]. In this study, we observed that the MPEP-induced expression of CHOP, GRP78 and GRP96 was attenuated by the $Ca^{2+}$ chelator BAPTA-AM in BV-2 cells, suggesting that the ER-stress, caused upon mGluR5 inhibition, was dependent on increased $[Ca^{2+}]_i$.

Impaired AMPK signaling has been associated with ER-stress in different cell types [36,38,70]. We found that the MPEP-mediated induction of ER-stress markers was potentiated by the AMPK inhibitor compound C and diminished by the activator AICAR. Importantly, pretreatment of BV-2 cells with either compound C or

AICAR did not affect the MPEP-dependent increase in $[Ca^{2+}]_i$ (data not shown), suggesting that the $Ca^{2+}$ release from the ER precedes ATP depletion and AMPK activation. The protective effects of pretreatment of cells with AICAR may be explained by an increased cytoplasmic ATP concentration, which may facilitate energy dependent transport of $Ca^{2+}$ back into the ER following mGluR5 blockade.

The MPEP-dependent increase in $[Ca^{2+}]_i$ and subsequent induction of ER-stress markers and mitochondrial dysfunction involved the activation of PLC and could be prevented by pretreatment of BV-2 cells with the PLC inhibitor U-73122. Importantly, an increased PLC activity could be measured following incubation of microglia with MPEP, suggesting that mGluR5 inhibition caused cellular stress via the excessive activation of the PLC-$IP_3$ pathway. It was reported that the mGluR5 agonist CHPG reduced the LPS-dependent inflammatory response and activated PLC, thereby increasing $[Ca^{2+}]_i$ in microglia [10]. Thus, a tight control of the balance of mGluR5 signaling is important to avoid cellular stress. Additionally, mGluR5 might cross regulate toll-like receptors, thereby resulting in a muted inflammatory response.

Classically, the activation of PLC resulting in the synthesis of $IP_3$ and the release of $Ca^{2+}$ from the ER was associated with Gq-coupled receptors [39]. In the present study, the MPEP-induced increase in $[Ca^{2+}]_i$ was attenuated by the Gi-protein inhibitor PTX, the PLC inhibitor U-73122 and the $IP_3R$ antagonist xestospongin C, thus suggesting crosstalk between mGluR5 receptors and Gi-protein subunits to modulate PLC and induce $IP_3R$-mediated $Ca^{2+}$ release from the ER. Several studies in a variety of cells and tissues demonstrated an increase in $[Ca^{2+}]_i$ following stimulation of Gi-coupled receptors [39,71,72]. For instance, treatment of natural killer cells with PTX diminished intracellular $Ca^{2+}$ influx and chemotaxis induced by oxidized lipids and lysophosphatidylcholine [72]. Further, PTX completely blocked the $Ca^{2+}$ responses induced by the endogenous µ-opioid receptor agonist endomorphin-1 in astrocytes [73].

## Conclusions
The present study demonstrates for the first time that antagonism of mGluR5 in BV-2 microglia results in increased cellular stress with mitochondrial dysfunction and ER-stress caused by an activation of PTX-sensitive Gi-proteins and subsequent PLC activation and $IP_3$-dependent $Ca^{2+}$ release from the ER. The increase in $[Ca^{2+}]_i$ upon inhibition of mGluR5 was followed by a depletion of cellular ATP and activation of AMPK, resulting in the induction of pro-inflammatory mediators. The results suggest that xenobiotics inhibiting mGluR5 disrupt $Ca^{2+}$ signaling and redox regulation in microglia, thereby promoting neuroinflammation.

## Additional file

Additional file 1: Table S1. Oligonucleotide primers for real-time PCR.

**Abbreviations**
$[Ca^{2+}]_i$: intracellular free $Ca^{2+}$; AMPK: AMP-dependent protein kinase; CHOP: transcriptional factor C/EBP homologous protein; CHPG: (RS)-2-chloro-5-hydroxyphenylglycine; DEPC: diethylpyrocarbonate; DHE: dihydroethidium; DMEM: Dulbecco's modified Eagle's medium; ELISA: enzyme-linked immunosorbent assay; ER: endoplasmic reticulum; GPCR: G-protein-coupled receptor; GAPDH: glyceraldehyde 3-phosphate dehydrogenase; GPCR: G-protein-coupled receptor; GRP78: glucose-regulated protein 78; GRP94: glucose-regulated protein 94; HBSS: Hank's balanced salt solution; HEPES: 4-(2-hydroxyethyl)-1-piperazineethanesulfonic acid; IL-6: interleukin-6; iNOS: inducible nitric oxide synthase; $IP_3$: inositol triphosphate; $IP_3R$: inositol triphosphate-induced receptor; LPS: lipopolysaccharide; MAPKs: mitogen-activated protein kinases; mGluR5: metabotropic glutamate receptor 5; MPEP: 2-methyl-6-(phenylethynyl)-pyridine; NEAA: non-essential amino acids; NF-κB: nuclear factor kappaB; NO: nitric oxide; NOX-2: NADPH oxidase type 2; PBA: sodium phenylbutyrate; PBS: phosphate-buffered saline; PCR: polymerase chain reaction; PDVF: polyvinylidene difluoride; PERK: PKR-like ER kinase; PKC: protein kinase C; PLC: phospholipase C; PTX: pertussis toxin; RIPA: radio immunoprecipitation assay; ROS: reactive oxygen species; RNS: reactive nitrogen species; RyR: ryanodine receptor; SDS-PAGE: sodium dodecyl sulfate-polyacrylamide gel electrophoresis; TBS: Tris-buffered saline; TBS-T: Tris-buffered saline with Tween; TNF: tumor necrosis factor; UPR: unfolded protein response.

**Competing interests**
The authors declare that they have no competing interests.

**Authors' contributions**
BC and AO designed the study. BC performed the experiments and analyzed the data. DK and AL helped planning experiments and analyzing the data. BC, DK, AL and AO wrote the manuscript. All authors read and approved the final manuscript.

**Author details**
[1]Division of Molecular and Systems Toxicology, Department of Pharmaceutical Sciences, University of Basel, Klingelbergstrasse 50, 4056 Basel, Switzerland. [2]Current address: Department of Preclinical Science and Applied Animal Science, Faculty of Veterinary Science, Mahidol University, Phutthamonthon, Nakhonpathom, Thailand.

**References**
1. Block ML, Zecca L, Hong JS: **Microglia-mediated neurotoxicity: uncovering the molecular mechanisms.** *Nat Rev Neurosci* 2007, **8**:57–69.
2. Ferraguti F, Shigemoto R: **Metabotropic glutamate receptors.** *Cell Tissue Res* 2006, **326**:483–504.
3. Byrnes KR, Loane DJ, Faden AI: **Metabotropic glutamate receptors as targets for multipotential treatment of neurological disorders.** *Neurotherapeutics* 2009, **6**:94–107.
4. Pajoohesh-Ganji A, Byrnes KR: **Novel neuroinflammatory targets in the chronically injured spinal cord.** *Neurotherapeutics* 2011, **8**:195–205.
5. Conn PJ, Pin JP: **Pharmacology and functions of metabotropic glutamate receptors.** *Annu Rev Pharmacol Toxicol* 1997, **37**:205–237.
6. Biber K, Laurie DJ, Berthele A, Sommer B, Tolle TR, Gebicke-Harter PJ, van Calker D, Boddeke HW: **Expression and signaling of group I metabotropic glutamate receptors in astrocytes and microglia.** *J Neurochem* 1999, **72**:1671–1680.

7. Wang JW, Wang HD, Zhong WZ, Li N, Cong ZX: **Expression and cell distribution of metabotropic glutamate receptor 5 in the rat cortex following traumatic brain injury.** *Brain Res* 2012, **1464**:73–81.

8. Wang JW, Wang HD, Cong ZX, Zhang XS, Zhou XM, Zhang DD: **Activation of metabotropic glutamate receptor 5 reduces the secondary brain injury after traumatic brain injury in rats.** *Biochem Biophys Res Commun* 2013, **430**:1016–1021.

9. Byrnes KR, Loane DJ, Stoica BA, Zhang J, Faden AI: **Delayed mGluR5 activation limits neuroinflammation and neurodegeneration after traumatic brain injury.** *J Neuroinflammation* 2012, **9**:43.

10. Byrnes KR, Stoica B, Loane DJ, Riccio A, Davis MI, Faden AI: **Metabotropic glutamate receptor 5 activation inhibits microglial associated inflammation and neurotoxicity.** *Glia* 2009, **57**:550–560.

11. Byrnes KR, Stoica B, Riccio A, Pajoohesh-Ganji A, Loane DJ, Faden AI: **Activation of metabotropic glutamate receptor 5 improves recovery after spinal cord injury in rodents.** *Ann Neurol* 2009, **66**:63–74.

12. Loane DJ, Stoica BA, Byrnes KR, Jeong W, Faden AI: **Activation of mGluR5 and inhibition of NADPH oxidase improves functional recovery after traumatic brain injury.** *J Neurotrauma* 2013, **30**:403–412.

13. Loane DJ, Stoica BA, Pajoohesh-Ganji A, Byrnes KR, Faden AI: **Activation of metabotropic glutamate receptor 5 modulates microglial reactivity and neurotoxicity by inhibiting NADPH oxidase.** *J Biol Chem* 2009, **284**:15629–15639.

14. Mead EL, Mosley A, Eaton S, Dobson L, Heales SJ, Pocock JM: **Microglial neurotransmitter receptors trigger superoxide production in microglia; consequences for microglial-neuronal interactions.** *J Neurochem* 2012, **121**:287–301.

15. Hu S, Sheng WS, Schachtele SJ, Lokensgard JR: **Reactive oxygen species drive herpes simplex virus (HSV)-1-induced proinflammatory cytokine production by murine microglia.** *J Neuroinflammation* 2011, **8**:123.

16. Kacimi R, Giffard RG, Yenari MA: **Endotoxin-activated microglia injure brain derived endothelial cells via NF-kappaB, JAK-STAT and JNK stress kinase pathways.** *J Inflammation* 2011, **8**:7.

17. Ibrahim AS, El-Remessy AB, Matragoon S, Zhang W, Patel Y, Khan S, Al-Gayyar MM, El-Shishtawy MM, Liou GI: **Retinal microglial activation and inflammation induced by amadori-glycated albumin in a rat model of diabetes.** *Diabetes* 2011, **60**:1122–1133.

18. Peterson LJ, Flood PM: **Oxidative stress and microglial cells in Parkinson's disease.** *Mediators Inflamm* 2012, **2012**:401264.

19. Filosto M, Scarpelli M, Cotelli MS, Vielmi V, Todeschini A, Gregorelli V, Tonin P, Tomelleri G, Padovani A: **The role of mitochondria in neurodegenerative diseases.** *J Neurol* 2011, **258**:1763–1774.

20. Federico A, Cardaioli E, Da Pozzo P, Formichi P, Gallus GN, Radi E: **Mitochondria, oxidative stress and neurodegeneration.** *J Neurol Sci* 2012, **322**:254–262.

21. Hardie DG: **AMP-activated protein kinase: an energy sensor that regulates all aspects of cell function.** *Genes Dev* 2011, **25**:1895–1908.

22. Ronnett GV, Ramamurthy S, Kleman AM, Landree LE, Aja S: **AMPK in the brain: its roles in energy balance and neuroprotection.** *J Neurochem* 2009, **109**(Suppl 1):17–23.

23. Cardaci S, Filomeni G, Ciriolo MR: **Redox implications of AMPK-mediated signal transduction beyond energetic clues.** *J Cell Sci* 2012, **125**:2115–2125.

24. Garcia-Gil M, Pesi R, Perna S, Allegrini S, Giannecchini M, Camici M, Tozzi MG: **5'-aminoimidazole-4-carboxamide riboside induces apoptosis in human neuroblastoma cells.** *Neuroscience* 2003, **117**:811–820.

25. Kuznetsov JN, Leclerc GJ, Leclerc GM, Barredo JC: **AMPK and Akt determine apoptotic cell death following perturbations of one-carbon metabolism by regulating ER stress in acute lymphoblastic leukemia.** *Mol Cancer Ther* 2011, **10**:437–447.

26. Zhang J, Xie Z, Dong Y, Wang S, Liu C, Zou MH: **Identification of nitric oxide as an endogenous activator of the AMP-activated protein kinase in vascular endothelial cells.** *J Biol Chem* 2008, **283**:27452–27461.

27. Ikeda M, Tsuno S, Sugiyama T, Hashimoto A, Yamoto K, Takeuchi K, Kishi H, Mizuguchi H, Kohsaka SI, Yoshioka T: **Ca spiking activity caused by the activation of store-operated Ca channels mediates TNF-alpha release from microglial cells under chronic purinergic stimulation.** *Biochim Biophys Acta* 2013, **1833**:2573–2585.

28. Noda M, Ifuku M, Mori Y, Verkhratsky A: **Calcium influx through reversed NCX controls migration of microglia.** *Adv Exp Med Biol* 2013, **961**:289–294.

29. Zou J, Vetreno RP, Crews FT: **ATP-P2X7 receptor signaling controls basal and TNFalpha-stimulated glial cell proliferation.** *Glia* 2012, **60**:661–673.

30. Eichhoff G, Brawek B, Garaschuk O: **Microglial calcium signal acts as a rapid sensor of single neuron damage** *in vivo. Biochim Biophys Acta* 2011, **1813**:1014–1024.

31. Brawek B, Garaschuk O: **Microglial calcium signaling in the adult, aged and diseased brain.** *Cell Calcium* 2013, **53**:159–169.

32. Foskett JK, White C, Cheung KH, Mak DO: **Inositol trisphosphate receptor Ca2+ release channels.** *Physiol Rev* 2007, **87**:593–658.

33. Sammels E, Parys JB, Missiaen L, De Smedt H, Bultynck G: **Intracellular Ca2+ storage in health and disease: a dynamic equilibrium.** *Cell Calcium* 2010, **47**:297–314.

34. Hacki J, Egger L, Monney L, Conus S, Rosse T, Fellay I, Borner C: **Apoptotic crosstalk between the endoplasmic reticulum and mitochondria controlled by Bcl-2.** *Oncogene* 2000, **19**:2286–2295.

35. Sano R, Reed JC: **ER stress-induced cell death mechanisms.** *Biochim Biophys Acta* 2013, **1833**:3460–3470.

36. Park YJ, Ko JW, Jang Y, Kwon YH: **Activation of AMP-activated protein kinase alleviates homocysteine-mediated neurotoxicity in SH-SY5Y cells.** *Neurochem Res* 2013, **38**:1561–1571.

37. Maria DA, de Souza JG, Morais KL, Berra CM, Zampolli Hde C, Demasi M, Simons SM, de Freitas SR, Chammas R, Chudzinski-Tavassi AM: **A novel proteasome inhibitor acting in mitochondrial dysfunction, ER stress and ROS production.** *Invest New Drugs* 2013, **31**:493–505.

38. Yang L, Sha H, Davisson RL, Qi L: **Phenformin activates the unfolded protein response in an AMP-activated protein kinase (AMPK)-dependent manner.** *J Biol Chem* 2013, **288**:13631–13638.

39. Rhee SG: **Regulation of phosphoinositide-specific phospholipase C.** *Annu Rev Biochem* 2001, **70**:281–312.

40. Woo MS, Park JS, Choi IY, Kim WK, Kim HS: **Inhibition of MMP-3 or -9 suppresses lipopolysaccharide-induced expression of proinflammatory cytokines and iNOS in microglia.** *J Neurochem* 2008, **106**:770–780.

41. Henn A, Lund S, Hedtjarn M, Schrattenholz A, Porzgen P, Leist M: **The suitability of BV2 cells as alternative model system for primary microglia cultures or for animal experiments examining brain inflammation.** *ALTEX* 2009, **26**:83–94.

42. Blasi E, Barluzzi R, Bocchini V, Mazzolla R, Bistoni F: **Immortalization of murine microglial cells by a v-raf/v-myc carrying retrovirus.** *J Neuroimmunol* 1990, **27**:229–237.

43. Livak KJ, Schmittgen TD: **Analysis of relative gene expression data using real-time quantitative PCR and the 2(-Delta Delta C(T)) method.** *Methods* 2001, **25**:402–408.

44. Muehlschlegel S, Sims JR: **Dantrolene: mechanisms of neuroprotection and possible clinical applications in the neurointensive care unit.** *Neurocrit Care* 2009, **10**:103–115.

45. Lea PM, Movsesyan VA, Faden AI: **Neuroprotective activity of the mGluR5 antagonists MPEP and MTEP against acute excitotoxicity differs and does not reflect actions at mGluR5 receptors.** *Br J Pharmacol* 2005, **145**:527–534.

46. Cosford ND, Tehrani L, Roppe J, Schweiger E, Smith ND, Anderson J, Bristow L, Brodkin J, Jiang X, McDonald I, Rao S, Washburn M, Varney MA: **3-[(2-Methyl-1,3-thiazol-4-yl) ethynyl]-pyridine: a potent and highly selective metabotropic glutamate subtype 5 receptor antagonist with anxiolytic activity.** *J Med Chem* 2003, **46**:204–206.

47. Mathiesen JM, Svendsen N, Brauner-Osborne H, Thomsen C, Ramirez MT: **Positive allosteric modulation of the human metabotropic glutamate receptor 4 (hmGluR4) by SIB-1893 and MPEP.** *Br J Pharmacol* 2003, **138**:1026–1030.

48. O'Leary DM, Movsesyan V, Vicini S, Faden AI: **Selective mGluR5 antagonists MPEP and SIB-1893 decrease NMDA or glutamate-mediated neuronal toxicity through actions that reflect NMDA receptor antagonism.** *Br J Pharmacol* 2000, **131**:1429–1437.

49. Sarnico I, Boroni F, Benarese M, Sigala S, Lanzillotta A, Battistin L, Spano P, Pizzi M: **Activation of NF-kappaB p65/c-Rel dimer is associated with neuroprotection elicited by mGlu5 receptor agonists against MPP(+) toxicity in SK-N-SH cells.** *J Neural Transm* 2008, **115**:669–676.

50. D'Antoni S, Berretta A, Seminara G, Longone P, Giuffrida-Stella AM, Battaglia G, Sortino MA, Nicoletti F, Catania MV: **A prolonged pharmacological blockade of type-5 metabotropic glutamate receptors protects cultured spinal cord motor neurons against excitotoxic death.** *Neurobiol Dis* 2011, **42**:252–264.

51. Vernon AC, Zbarsky V, Datla KP, Croucher MJ, Dexter DT: **Subtype selective antagonism of substantia nigra pars compacta group I metabotropic**

glutamate receptors protects the nigrostriatal system against 6-hydroxydopamine toxicity in vivo. J Neurochem 2007, **103**:1075–1091.

52. Hoffmann A, Kann O, Ohlemeyer C, Hanisch UK, Kettenmann H: Elevation of basal intracellular calcium as a central element in the activation of brain macrophages (microglia): suppression of receptor-evoked calcium signaling and control of release function. J Neurosci 2003, **23**:4410–4419.

53. Li X, Cudaback E, Keene CD, Breyer RM, Montine TJ: Suppressed microglial E prostanoid receptor 1 signaling selectively reduces tumor necrosis factor alpha and interleukin 6 secretion from toll-like receptor 3 activation. Glia 2011, **59**:569–576.

54. Korotzer AR, Whittemore ER, Cotman CW: Differential regulation by beta-amyloid peptides of intracellular free Ca2+ concentration in cultured rat microglia. Eur J Pharmacol 1995, **288**:125–130.

55. McLarnon JG, Choi HB, Lue LF, Walker DG, Kim SU: Perturbations in calcium-mediated signal transduction in microglia from Alzheimer's disease patients. J Neurosci Res 2005, **81**:426–435.

56. Lee S, Kim YK, Shin TY, Kim SH: Neurotoxic effects of bisphenol AF on calcium-induced ROS and MAPKs. Neurotox Res 2013, **23**:249–259.

57. Wang X, Chen S, Ma G, Ye M, Lu G: Involvement of proinflammatory factors, apoptosis, caspase-3 activation and Ca2+ disturbance in microglia activation-mediated dopaminergic cell degeneration. Mech Ageing Dev 2005, **126**:1241–1254.

58. Huang X, Zhai D, Huang Y: Study on the relationship between calcium-induced calcium release from mitochondria and PTP opening. Mol Cell Biochem 2000, **213**:29–35.

59. Ichas F, Jouaville LS, Mazat JP: Mitochondria are excitable organelles capable of generating and conveying electrical and calcium signals. Cell 1997, **89**:1145–1153.

60. Brookes PS, Yoon Y, Robotham JL, Anders MW, Sheu SS: Calcium, ATP, and ROS: a mitochondrial love-hate triangle. Am J Physiol Cell Physiol 2004, **287**:C817–C833.

61. Deng YY, Lu J, Ling EA, Kaur C: Role of microglia in the process of inflammation in the hypoxic developing brain. Front Biosci 2011, **3**:884–900.

62. Ferger AI, Campanelli L, Reimer V, Muth KN, Merdian I, Ludolph AC, Witting A: Effects of mitochondrial dysfunction on the immunological properties of microglia. J Neuroinflammation 2010, **7**:45.

63. Moss DW, Bates TE: Activation of murine microglial cell lines by lipopolysaccharide and interferon-gamma causes NO-mediated decreases in mitochondrial and cellular function. Eur J Neurosci 2001, **13**:529–538.

64. Nam HG, Kim W, Yoo DY, Choi JH, Won MH, Hwang IK, Jeong JH, Hwang HS, Moon SM: Chronological changes and effects of AMP-activated kinase in the hippocampal CA1 region after transient forebrain ischemia in gerbils. Neurol Res 2013, **35**:395–405.

65. Giri S, Nath N, Smith B, Viollet B, Singh AK, Singh I: 5-aminoimidazole-4-carboxamide-1-beta-4-ribofuranoside inhibits proinflammatory response in glial cells: a possible role of AMP-activated protein kinase. J Neurosci 2004, **24**:479–487.

66. Lu DY, Tang CH, Chen YH, Wei IH: Berberine suppresses neuroinflammatory responses through AMP-activated protein kinase activation in BV-2 microglia. J Cell Biochem 2010, **110**:697–705.

67. Sauer H, Engel S, Milosevic N, Sharifpanah F, Wartenberg M: Activation of AMP-kinase by AICAR induces apoptosis of DU-145 prostate cancer cells through generation of reactive oxygen species and activation of c-Jun N-terminal kinase. Int J Oncol 2012, **40**:501–508.

68. Labuzek K, Liber S, Gabryel B, Okopien B: AICAR (5-aminoimidazole-4-carboxamide-1-beta-4-ribofuranoside) increases the production of toxic molecules and affects the profile of cytokines release in LPS-stimulated rat primary microglial cultures. Neurotoxicology 2010, **31**:134–146.

69. Kim WH, Lee JW, Suh YH, Lee HJ, Lee SH, Oh YK, Gao B, Jung MH: AICAR potentiates ROS production induced by chronic high glucose: roles of AMPK in pancreatic beta-cell apoptosis. Cell Signal 2007, **19**:791–805.

70. Salvado L, Coll T, Gomez-Foix AM, Salmeron E, Barroso E, Palomer X, Vazquez-Carrera M: Oleate prevents saturated-fatty-acid-induced ER stress, inflammation and insulin resistance in skeletal muscle cells through an AMPK-dependent mechanism. Diabetologia 2013, **56**:1372–1382.

71. Jiang H, Kuang Y, Wu Y, Smrcka A, Simon MI, Wu D: Pertussis toxin-sensitive activation of phospholipase C by the C5a and fMet-Leu-Phe receptors. J Biol Chem 1996, **271**:13430–13434.

72. Rolin J, Al-Jaderi Z, Maghazachi AA: Oxidized lipids and lysophosphatidyl-choline induce the chemotaxis and intracellular calcium influx in natural killer cells. Immunobiology 2013, **218**:875–883.

73. Block L, Forshammar J, Westerlund A, Bjorklund U, Lundborg C, Biber B, Hansson E: Naloxone in ultralow concentration restores endomorphin-1-evoked Ca(2)(+) signaling in lipopolysaccharide pretreated astrocytes. Neuroscience 2012, **205**:1–9.